Available online at www.sciencedirect.com

Food and Bioproducts Processing

journal homepage: www.elsevier.com/locate/fbp

Continuous ethanol production via ultrasound-enhanced yeast sedimentation

Carlos Domingo-Félez, Katarzyna Jankowska, Ioannis V. Skiadas, John M. Woodley, Manuel Pinelo *

Department of Chemical Engineering, Technical University of Denmark, Søltofts Plads 228A, 2800 Kgs. Lyngby, Denmark

ARTICLE INFO

Article history:
Received 28 November 2022
Received in revised form 24 March 2023
Accepted 7 June 2023
Available online 9 June 2023

Keywords:
Ultrasound
RSM
Ethanol
Yeast

ABSTRACT

Continuous glucose fermentation produces bioethanol at higher volumetric rates than conventional batch or fed-batch systems. The retention of yeast cells via ultrasonic sedimentation in a lab-scale fermenter allowed for shearless, continuous cell upconcentration, and consequently process intensification. The cell separation efficiency of the ultrasonic system was predicted with a Response Surface Model (RSM) developed for yeast cells based on the linear, mixed, and quadratic effects of the operating variables and flow rates (3 levels, 5 variables). The experiments for the RSM calibration were designed via a central composite design. The efficiency model was validated and showed dependency to the Biomass concentration, Power input, and Harvest rate ($R^2_{calibration}$ = 0.92, $R^2_{prediction}$ = 0.83). A lab-scale fermenter fed with yeast growth medium was operated at varying dilution rates (0.1 – 0.6 h^{-1}) based on the RSM to maximize the cell retention efficiency (23%–90%). Yeast cell concentration in the fermenter reached up to 31.5 ± 0.7 g/L while it remained at around 3 g/L in the harvest stream for all the dilution rates tested. The ethanol concentration ranged between 17 and 23 g/L and reached high volumetric productivity (8.8 g/L/h). A control run without ultrasonic sedimentation led to the washout of biomass at a dilution rate of 0.6 h^{-1}. Ultrasonic yeast sedimentation is a promising technology for cell retention and enhanced productivity in continuous fermentation processes.

1. Introduction

Fermentation processes are carried out as batch, fed-batch or continuous in the industrial scale (Li et al., 2011; Rahimi et al., 2019), depending on the efficiency of the specific fermentation process and the available equipment. Interest in continuous fermentation has grown due to the advantages over batch and fed-batch processes. The effective fermentation time of *Yarrowia lipolytica* was 27 h shorter using continuous operation compared to fed-batch fermentation (Xie et al., 2017), whereas the productivity of poly-3-hydroxybutyrate production increased from 0.18 g/L/h in batch to 0.33 g/L/h in continuous mode (Ling et al., 2018). Moreover, from the industrial point of view the continuous fermentation seems to be an ideal process in terms of constant control of pH, temperature, agitation, and aeration while sustaining the productivity of desired compounds (Li et al., 2014). On the other hand, continuous process has some disadvantages. The possibility of contamination due to continuous feed and extended operation periods. Furthermore, continuous fermentation process usually requires more complex apparatus that allow for continuous feed of fresh medium and at the same time, harvesting of cells, used medium, and obtained product (Li et al., 2014). Nevertheless, continuous processes seem to be

* Corresponding author.
E-mail address: mp@kt.dtu.dk (M. Pinelo).
https://doi.org/10.1016/j.fbp.2023.06.002

the most appropriate operation in production of valuables compounds by fermentation.

The production of bioethanol from a variety of feeds such as sugars, starch, lignocellulosic or algal biomass is a well-studied fermentation process (Balat, 2011; Mohd Azhar et al., 2017; Tse et al., 2021). The significance of bioethanol as biofuel results from a growing consumption of energy and pollution of environment caused by combustion of fossils fuels, therefore the optimization of bioethanol production and increase in productivity remains relevant. Bioethanol production using suspended yeast cells is inefficient due to the higher cost of cell recycling (Kumar et al., 2011). Brandberg et al. (2007) compared three methods of cell retention of *Saccharomyces cerevisiae* ATCC 96581: filtration, sedimentation, and immobilization in calcium alginate (Brandberg et al., 2007). Although every method improved the volumetric ethanol production, only the immobilization method could operate at dilution rates higher than 0.2 h^{-1}. An external microfiltration membrane module was tested on *S. cerevisiae* NCIM 3095 cells, but the decreasing flux limited the performance with a low cell density of 2.4 g/L (Saha et al., 2019). Physical growth support retains cells in the fermenter efficiently. *Saccharomyces cerevisiae* M30 cells attached to silk cocoons grew up to 44.5 g/L, yielding a very high bioethanol productivity of 19.0 g/L/h, 12.6-fold higher than in batch mode (optimum dilution rate of 0.36 h^{-1}) (Rattanapan et al., 2011). Considering sugar-cane stalks as growth support, the highest reported so far productivity of 29.6 g/L/h was achieved, at a dilution rate of 0.83 h^{-1} and 86% sugar utilization, but reached up to 1.5 h^{-1} under stable operation (de Vasconcelos et al., 2004).

Alternative methods of physical cell retention are still being sought, such as acoustofluidic separation of cells and particles. Under the action of ultrasonic standing waves the motion of particles in a liquid is predictable, where particles are affected by ultrasonic radiation and streaming forces (Wu et al., 2019). From a homogenous particle suspension, a continuous phase from high-frequency ultrasounds (≈ 2 MHz) aggregates cells based on differences in compressibility and density in nodal and anti-nodal planes (Luo et al., 2018). This method of particle separation has been used in medical field to separate specific blood components (Wu et al., 2017), to filtrate bacteria and yeast (Hawkes et al., 1997), or to harvest microalgae (Bosma et al., 2003). The cell retention time is increased, and therefore the cell concentration, compared to the liquid retention time. Apart from the lack of shear stress on cells compared to membrane filtrations, the viability remains unchanged after exposure to an ultrasonic field for plant cells (Shin et al., 1999) and yeast (Palme et al., 2010; Radel et al., 2000). The continuous exposure to an ultrasonic field at lower frequencies (20 – 40 kHz) affects the microbial growth and enzyme activity, both enhancing and inhibiting ethanol productivity (He et al., 2021; Singh et al., 2015; Huezo et al., 2019). The potential benefits of ultrasonic yeast cell separation are the operation at higher than the maximum specific growth rate, the lack of shear stress on cells, and the possibility of long-term continuous operation. We hypothesize that the application of this unexplored technology for yeast cells will enhance the fermentation productivity which, to our knowledge, has never been reported.

Our objective is to: (i) study the feasibility of ultrasonic yeast cell separation for continuous fermentation processes, with the case study of bioethanol production, and (ii) develop a cell separation efficiency model to predict the interactions between actuators in an ultrasonic separation lab-scale setup.

2. Materials and methods

2.1. *Cell separation efficiency model*

2.1.1. *Experimental design for the concentration separation Response Surface Model*

A statistical experimental design was selected to optimize the multivariable process. The central composite design was selected over the Box-Behnken design as the location of the optimum was unknown (Bosma et al., 2003).

The design was built and analysed with the software Matlab 2020b (The Mathworks Inc., Natick, USA). Three levels were defined for the five variables and the centre of the experimental domain was measured ten times to estimate the repeatability (central composite face-centred, CCF (5, *faced*), n = 36, three blocks) (Table 1, SI.1). The low and high levels of coded variables Biomass concentration (X_1) were defined based on literature values (Kumar et al., 2011; Rattanapan et al., 2011; Fan et al., 2014), and the Recirculation rate (X_2) and Harvest rate (X_3) were defined by targeted dilution rates (0.1–0.6 h^{-1}). Coded variables Time ON (X_4) (duration of ultrasonic field), and ultrasonic Power field input (X_5) were not symmetric due to instrumental limitations (discontinuous values for X_4 = 1, 2, 3, 5, 10, and X_5 = 2, 3, 5, 7, 10).

The response considered the concentration separation efficiency (Y) as the ratio between the concentrations in the harvest and in the fermenter (Eq. (1)).

$$\text{Efficiency} = 1 - C_{Harvest}/C_{Fermenter} \quad (1)$$

The separation efficiency in mass flow was also analysed but model responses did not differ (SI.2). The efficiency was fitted to a polynomial equation (Eq. (2)).

$$Y = b_0 + \sum_{i=1}^{5} b_i X_i + \sum_{i=1}^{5}\sum_{j=1}^{5} b_{ij} X_i X_j + \sum_{ii=1}^{5} b_{ii} X_i^2 \quad (2)$$

The parameters b correspond to the polynomial coefficients: b_0 is the intercept term, b_i the main effects, b_{ij} ($i \neq j$) the interaction effects between the parameters, and b_{ii} the square effects.

To distinguish statistical significant coefficients the method of backward stepwise elimination was followed based on Bosma et al., (2003). Briefly, coefficients with a probability value (p-value) higher than 0.10 were considered noise signals. Initially, all 21 coefficients were considered, and the coefficient with the highest probability value was removed. The process continued iteratively until only significant coefficients remained ($p < 0.10$). Additional experiments performed at

Table 1 – Levels of variables in the central composite design for the ultrasonic-assisted yeast cell separation Response Surface Model.

Variable	Unit	Coded variable	Low level (–1)	Medium level (0)	High level (+1)
Biomass	g/L	X_1	20	45	70
Recirculation	L/d	X_2	55	77	98
Harvest	L/d	X_3	4.8	10.6	16.4
Time ON	min	X_4	1	5	10
Power	W	X_5	2	5	10

different X_i values from CCF than shown in Table 1 were considered for model validation (n = 28, SI.2).

2.1.2. *Experimental setup and analytical procedures*

A BioBench fermenter (Biostream, Netherlands) was operated in closed loop mode (working volume ≤ 10 L). Commercially available freeze-dried yeast cells were re-suspended in tap water to the desired concentration and the suspension was mixed mechanically (300 rpm) and via air supply (0.5 LPM). The cell concentration was determined by dry weight measurements and correlated to the values of the absorbance at 600 nm (X_1) (SI.2). The cell size was measured with the ParticleTech Analyzer (ParticleTech ApS, Denmark). The recirculation rate from the fermenter to the ultrasonic chamber and the harvest flow rate were controlled via peristaltic pumps (X_2, X_3) (Fig. 1). An ultrasonic harvest chamber (Applikon, BioSep 50 L) was mounted on the top plate (volume = 50 mL) and connected to a control unit (BioSep APS 990). The control unit fixes the power, timer, and frequency of the power to the chamber (X_4, X_5, Time OFF constant at 5 s, and 2.1 MHz). The system operates semi-continuously with periods Time ON + Time OFF: during Time ON (X_4) the recirculation and harvest flow and the power is supplied to the chamber, and during Time OFF no power or flows allow for cells to settle faster from the chamber.

During one test at the desired cell concentration, the separation was operated for at least 20 min to reach steady-state before sampling for 10 min or 100 mL to avoid field cyclic variability (X_4 + 5 s Time OFF). The system was operated in closed loop mode, with the no influent flow and the harvest flow returned to the fermenter A gas trap prevented gas bubbles from entering the ultrasonic chamber and disrupting the flow field. The gas and excess liquid flow returned to the fermenter.

2.2. *Glucose fermentation: microorganism, medium and analytics*

Yeast cells were grown on yeast extract-peptone-dextrose (YPD) agar media consisting of per liter: 10 g yeast extract, 20 g peptone, 22 g glucose monohydrate, and 20 g agar. All chemicals were of pure analytical grade unless otherwise specified. The YPD medium used for the inoculums preparation and continuous operation was the same as for yeast cell growth except for agar, and the YPD concentrations were modified proportionally during continuous operation to adjust the glucose concentration. All the materials in the medium were sterilized separately in an autoclave at 121 °C for 20 min.

Inoculums were prepared by transferring a loopful of an isolated colony from an agar plate to a 500 mL Erlenmeyer flask containing 200 mL of inoculum media, cultivated in a shaking incubator at 30 °C and 100 rpm for 24 h. Continuous fermentation experiments were performed in the BioBench fermenter, at 33 °C, pH 5.0, and 300 rpm mixing, operated at an active volume of 4 L and dilution rates of 0.1, 0.2, 0.3 h^{-1} (glucose influent ≈ 45 g/L) and 0.4 h^{-1} (glucose influent ≈ 15 and 80 g/L). A control experiment was performed at 2 L active volume, 150 rpm mixing, and the highest dilution rate of 0.6 h^{-1} with ultrasonic field, and without ultrasonic field to investigate possible washout of biomass. For every dilution rate, or harvest rate (Table 1), the system was operated for at least 5 HRTs (Hydraulic Retention Times) before sampling for performance analysis.

Samples from the fermenter and harvest stream were withdrawn for analyses of cell concentration, residual glucose, ethanol, acetic acid, lactic acid and glycerol. Glucose and fermentation products were quantified on high performance liquid chromatography HPLC system HP 1100 (Agilent 1100) equipped with a BioRad Aminex HPX-87 H at 63 °C and a refractive index (RI) detector (RID 1362 A) using 0.6 mL/min of 12 mM H_2SO_4 as eluent. All samples were filtered through a 0.22 µm syringe filter prior to analysis.

3. Results

3.1. *Yeast cells separation efficiency: experimental and modelling results*

The concentration separation efficiency (Y) of the central composite experiments ranged between 15% and 99% (SI.1). During certain experimental conditions the control unit could not sustain a constant power or frequency output, which alligned to the supplier operation guidelines. Low power output was not stable at high cell concentrations (n9: X_1 (+1), X_5 (−1), Y = 0.525). At high power output very small air bubbles appeated in the chamber, yielding frequency fluctuations due to cavitation and affecting negatively the separation process (n26: X_5 (+1), Y = 0.302). At high separation efficiencies a cell blanket was visible through the ultrasonic chamber (glass walls) (Fig. 1), with the top section being the cell-free harvest and the thick bottom layer the return flow to the fermenter. The yeast cell size was measured at the

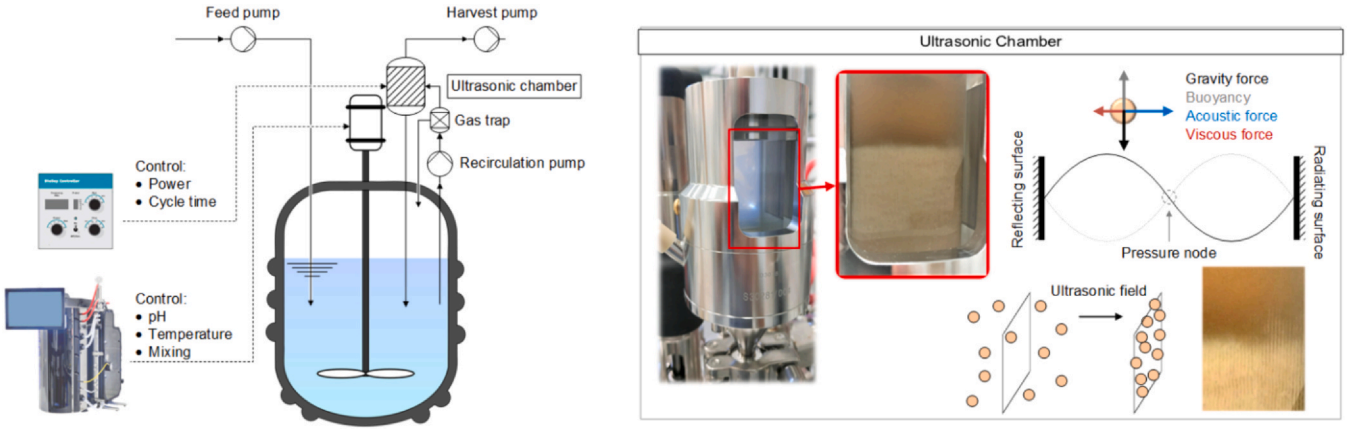

Fig. 1 – Ultrasonic yeast cell separation for continuous glucose fermentation (left). Picture of the ultrasonic chamber (empty), detail of the yeast cell blanket during operation, and forces acting on a particle under an ultrasonic field (right).

Table 2 – Coefficients of the concentration efficiency model.

Parameter	Variable	Value	Error	p-value
b_1	Constant	1.80	7%	4.8E-14
b_2	X1	-0.0115	11%	8.1E-10
b_4	X3	-0.148	18%	7.8E-06
b_6	X5	0.0852	40%	1.9E-02
b_{10}	X1·X5	0.000618	29%	2.0E-03
b_{15}	X3·X5	-0.00143	54%	7.6E-02
b_{19}	X3·X3	0.00522	22%	8.4E-05
b_{21}	X5·X5	-0.00794	33%	4.9E-03

beginning and end of the experiments, with an average value of 8.7 ± 1.1 µm (n = 8818) (SI.2).

From the initial 21 model parameters the model was stepwise reduced to 8 significant parameters (maximum p-value b_{15} = 0.08) (Table 2, SI.2). The R^2 value for the Efficiency model is 0.916, the adjusted R^2 is 0.895, and the prediction R^2 is 0.829, which indicates a good model fit (MSE = 0.0053, p-value = 2E-13, F = 43.6). The variables X_2 and X_4 (Recirculation, Time ON) do not affect the separation efficiency, X_1 (Biomass) has a linear and interaction effects, and X_3 and X_5 (Harvest, Power) have linear, interactions, and quadratic effects (Eq. (3), Table 2, SI.2). The low p-values for the linear Biomass (b_2), and linear and quadratic effect parameters of the Harvest rate (b_4, b_{19}), highlight the importance of Biomass and Harvest on the separation efficiency.

$$\text{Efficiency}(-) = b_1 + b_2\cdot\text{Biomass} + b_4\cdot\text{Harvest} + b_6 \cdot\text{Power} + b_{10}\cdot\text{Biomass}\cdot\text{Power} + b_{15}\cdot\text{Harvest} \cdot\text{Power} + b_{19}\cdot\text{Harvest}^2 + b_{21}\cdot\text{Power}^2 \quad (3)$$

The X_i values for additional experiments (SI.1) were evaluated with the Efficiency model (Eq. 3) for validation purposes showing a good model fit ($R^2_{validation}$ = 0.81, n = 28).

To explore the operational space of the variables affecting the separation efficiency the model was evaluated at the center values of the non-affecting variables X_2, X_4, and throughout low to high levels for variables X_1, X_3, X_5 (Fig. 2). The highest efficiencies (≈ 100%) are predicted at the lowest Harvest and Biomass values for mid-range Power levels (5 and 7 W). When the chamber is loaded with increasing number of cells (Biomass or Harvest), the efficiency decreases to 74% at 70 g/L, and to 69% at 6 L/d, as predicted by a higher contribution of the negative coefficients (b_2, b_4, and b_{15}) compared to the positive coefficients (b_{10}, b_{19}) (Table 2).

3.1.1. *Effect of measurement uncertainty and mass-based efficiency model*

The uncertainty in the Biomass concentration measurements (X_1, g/L) from the calibration between cell dry weight and 600 nm absorbance was propagated to the initial conditions of the calibration runs (SI.2). The model was re-evaluated for 1000 Monte Carlo samples including an assumed normal error. The average parameter models differed in less than 3.5% from the original run (SI.2), and the maximum coefficient of variation was 23%. Hence, the experimental error of biomass concentration values did not have a great effect on the RSM efficiency model output.

The cell separation efficiency was also calculated in mass units by multiplying cell concentrations with the corresponding flow rates instead of cell concentration (Eq. (1), SI.2) (Bosma et al., 2003). The model calibration process was repeated for the mass-based efficiency values and the same model structure (Eq. (3)) was obtained with different parameter values (SI.2).

3.2. *Continuous bioethanol production under ultrasound field cell separation*

The ultrasound field power of the cell retention chamber (X_5) was set based on the separation efficiency model prediction (Eq. (3)), with two inputs: the harvest rate (X_3), fixed by the dilution rate, and the measured cell concentration in the fermenter (X_1). The highest dilution rates tested (0.6 h^{-1}) were operated at a reduced volume (2 L) to prevent high harvest rates (X_3). For all the dilution rates tested the optimimum field power varied within the levels 5 and 7 W. Increasing dilution rates corresponded to higher glucose loadings, but the glucose feed concentration was not constant between dilution rates (Table 3, Fig. 3). At the dilution rate of 0.39 h^{-1} two glucose loadings were tested to study maximum glucose uptake rates and the effect of glucose feed on the cell concentration and separation efficiency.

Yeast cells concentrated up to 31.5 g/L at the lowest dilution rate, with a decreasing trend at higher dilution rates, highlighting the negative effect of the harvest rate (X_3) on the ultrasound separation efficiency (Table 3, Fig. 3). The cell concentration in the harvest did not vary significantly between 2.2 and 4.4 g/L. The cell separation efficiencies ranged

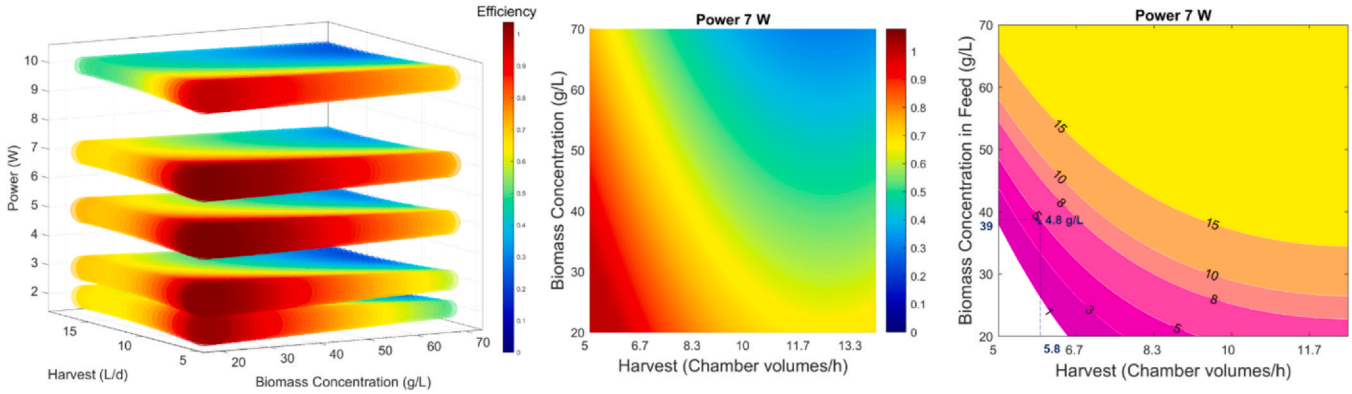

Fig. 2 – Model evaluation results for varying X_1, X_3, and X_5 values. Efficiency predictions are shown as colormap and bubble size (Left). Heatmap example of efficiency for Power = 7 W (Center), and corresponding Harvest isoconcentration contour map (Right). The Harvest rate is shown in L/d units and Chamber volumes/h for comparison with systems of different size.

Table 3 – Continuous fermentation: dilution and loading rates, ethanol productivity, and cell separation efficiencies.

Variable	Units							
Dilution rate	1/h	0.10	0.19	0.29	0.39	0.39	0.58	0.60*
Glucose - Feed concentraion	g/L	58 ± 1	45 ± 1	36 ± 1	14 ± 1	79 ± 0	37 ± 4	19 ± 1
Glucose - Loading rate	g/(L·h)	5.7 ± 0.1	8.8 ± 0.1	10.6 ± 0.2	5.5 ± 0.2	30.9 ± 0.0	21.3 ± 2.3	11.1 ± 0.6
Glucose - Uptake efficiency		98%	98%	98%	92%	82%	94%	9%
Ethanol - Productivity	g/(L·h)	2.2 ± 1.2	3.0 ± 1.0	5.0 ± 1.1	1.2 ± 0.2	8.8 ± 0.9	6.5 ± 0.4	0.7 ± 0.2
Cell concentration - Fermentor	g/L	31.5 ± 0.7	22.9 ± 3.3	15.6 ± 2.4	12.2 ± 1.7	20.9 ± 0.2	23.6 ± 8.6	2.2 ± 0.1
Cell concentration - Harvest	g/L	3.3 ± 0.1	2.2 ± 0.5	3.0 ± 0.2	2.4 ± 0.7	16.0 ± 0.5	4.4 ± 0.9	**
Cell separation efficiency		89%	90%	80%	80%	23%	81%	**

* Control, no ultrasound field power during 5 HRTs, ** Not applicable.

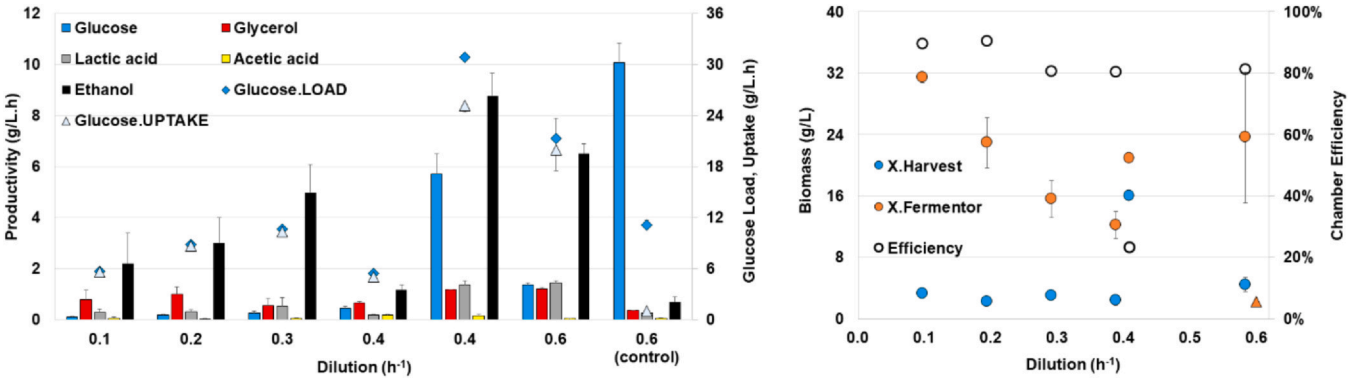

Fig. 3 – Continuous glucose fermentation. Left: Ethanol productivity (bars) at varying dilution rates, glucose load (diamond) and uptake (triangle) rates. Right: Biomass concentration in the fermenter (orange), harvest (blue), and chamber separation efficiency (empty) during ultrasound separation (circles), and control with no ultrasound separation (triangle).

between 80% and 90% for runs with high glucose uptake efficiency, which corresponds to low glucose concentration in the fermenter. Residual glucose indicates a higher specific activity that led to a higher specific gas production rate (CO_2). Small bubbles rising through the separation chamber disrupted the settling pattern which hamper the ultrasound separation. At an equal dilution rate (0.39 h^{-1}) a higher glucose loading (5.5 and 30.9 g/L/h) increased both the glucose concentration (1.2 and 14.6 g/L) and the cell concentration (12.2 and 20.9 g/L), but decreased the separation efficiency (80% and 23%) (Fig. 3). In the control run at the highest dilution rate (0.6 h^{-1}), the lack of the ultrasound separation resulted in the washing out of yeast cells which reached a concentration of only 2.2 g/L after 5 HRTs and a glucose uptake efficiency decreased to only 9% (SI.3).

The ethanol concentration remained at non-inhibitory levels for all the runs (< 23 g/L) (Zhang et al., 2015; Chen et al., 2005). The ethanol productivity increased with the dilution rate and glucose feed concentration, ranging from 1.2 to 8.8 g/L/h, except for the control run (0.7 g/L/h) (Fig. 3). The average mass product yields on glucose were 38 ± 6% for ethanol, 8 ± 4% for glycerol, 5 ± 1% for acetic acid, and 1 ± 0.2% for lactic acid. No significant trends were observed between product yields and dilution rates indicating comparable fermentation results ($p > 0.05$) (data not shown).

4. Discussion

4.1. *Ultrasonic separation of yeast cells*

Ultrasonic cell separation upconcentrates both eukaryotic and prokaryotic cells, with a higher efficiency for yeast compared to *E. coli* (Hawkes et al., 1997; Bosma et al., 2003). Plant cells (*Aloe saponaria*) accumulated up to 17 g/L (Shin et al., 1999), alga *Monodus subterraneus* was harvested at almost 21-fold concentration compared to the air-lift-loop reactor, and sophorolipids were separated from a 14 g/L solution of the yeast *Candida bombicola* (Palme et al., 2010). Hence, ultrasonication can yield high density cultures of yeast cells, but only linear and univariate effects of the actuators (X_1:X_5) have been studied previously (Hawkes and Coakley, 1996).

By simultaneously exploring the interactions between bioprocess (X_1, X_3) and ultrasonic variables (X_2, X_4, X_5), we propose a general RSM for yeast cultures constrained to the levels of the variables studied (Table 1). Briefly, the cell separation efficiency, or cell accumulation (X_1), is negatively affected by the harvest rate (X_3), and the power input (X_5) shows a maximum at 5–7 W. The recirculation rate (X_2) and the duration of the ultrasonic field (X_4) did not influence the separation efficiency significantly.

Overall, the ultrasonic system allows for process intensification by efficient yeast cell retention and consequently higher volumetric process rates. At low dilution (harvest) rates cells upconcentrate significantly, over 70-fold, and therefore the corresponding substrate conversion increases. For example, with cell concentrations of 20 and 45 g/L almost 99% separation efficiency was achieved at the lowest harvest rates (5.8 L/d). The corresponding harvest cell concentrations were below 0.3 and 0.6 g/L, which may be beneficial for further downstream processing steps. Although operating at higher dilution rates decreases the separation efficiency, it permits loadings exceeding the maximum specific growth rate.

The same commercial ultrasonic system was also characterized via RSM and harvested microalgae (Bosma et al., 2003). Differently to our proposed RSM in Eq. 3, neither the feed rate nor recirculation of the microalgae system showed a high impact on the efficiency, with a very small, and thus significant, p-value of the linear and square effect. However, the difference between recirculation and harvest did not influence the separation efficiency, which was reported as surprising, as when the chamber fills with cells the efficiency should drop. Similarly to this study, at high cell concentrations the ultrasonic field cannot capture all the cells, decreasing the process efficiency. The opposing results between the two systems can be attributed to: aggregation differences between microalgae and yeast, the cell concentration range studied, and different specific volumetric loadings (chamber of 7 mL compared to 50 mL).

4.2. *Continuous glucose fermentation under ultrasonic cell separation*

4.2.1. *Shearless cell retention under continuous operation*

Physical cell retention in surfaces or gels limits nutrient transport, and spatial substrate gradients can lead to varying growth type, as in biofilm systems. Ultrasonic sedimentation retains cells growing continuously in suspension without generating any shear stress as membrane filtration units do. Membrane modules operate in semi-continuous mode due to the need of backflush or membrane cleaning but yield a cell-free product stream. On the other hand, the ultrasonic system can operate under steady-state for longer periods of time than membrane modules but the product stream will contain the discharged microbial cells. When the fermentation starts, the relatively low number of cells may be retained easier but when the cell concentration reaches high values the separation efficiency decreases, as the acoustic chamber limits the sedimentation capacity and the system reaches equilibrium. Under steady-state part of the produced cells are discharged, which adds complexity to the downstream processes ($P_X = Y_{X/S} \cdot \Delta S$, g/L), where $Y_{X/S}$ is the biomass yield on substrate (g cell / g substrate), and ΔS the amount of substrate consumed (g/L).

In a continuous system, glucose consumption is incomplete and residual glucose corresponds to higher specific activity (Table 3, Fig. 3). The high fermentation rate created small bubbles (assumed to be of high CO_2 concentration), the majority of which were removed by a gas trap (Fig. 1). However, at high dilution rates (0.39, 0.58 h^{-1}) and lower glucose uptake rate efficiencies (82, 94%), the high rate of bubble production hampered the separation efficiency by rising through the sedimentation field and mixing the cell blanket (the hydraulic retention time in the acoustic chamber was less than 2 min, 1.3% of the total HRT).

4.2.2. *Bioethanol productivity*

The benefits in productivity of continuous fermentation with cell recycle compared to batch fermentation are well documented (Kumar et al., 2011). The main disadvantages claimed for continuous ethanol production are the high cost of cell recycling, the limitation of the dilution rate and the greater contamination risk as susceptible to environmental variations (Kumar et al., 2011). However, physical cell immobilization allows for high dilution rates, which compensates for the lower ethanol yield due to incomplete substrate consumption compared to batch processes (Sánchez and Cardona, 2008). Ultrasonic sedimentation overcomes some limitations by continuously operating at higher cell concentrations, independently of the dilution rate, even over the maximum specific growth rate, as shown by the biomass washout in the control run (Fig. 3).

To be of practical use in the industry, the ethanol productivity should be over 1 g/L/h, which benefits from the high yield and high tolerance to ethanol (> 100 g/L) (Zhang et al., 2011; Chang et al., 2018). Continuous fermentation reaches significantly higher productivities (SI.3). Embedding of *S. cerevisiae* cells in zeolite composite carriers and alginate retained yeast cells and achieved ethanol productivities of 6.6 g/L/h (Zheng et al., 2012). Similarly, cell retention in silk cocoons produced up to 19.0 g/L/h with a 76% sugar utilization (Rattanapan et al., 2011), and cell immbolization in sugarcane stalks achieved 29.6 g/L/h operating at high dilution rates (0.83 h^{-1}) (de Vasconcelos et al., 2004). The aim of the present study was not to maximize ethanol production but to characterize the feasibility of ultrasonic yeast sedimentation. Compared to literature, where the maximum rate was achieved when using sugars at approximately 150 g/L (Mohd Azhar et al., 2017), we operated at much lower glucose concentrations (Table 3). At a dilution rate of 0.39 h^{-1}, increasing the glucose feed concentration from 14 to 79 g/L lead to a productivity increase from 1.2 to 8.8 g/L/h due to a higher cell concentration in the fermenter (12.2 and 20.9 g/L). The increase in productivity resulted in a lower cell separation efficiency (80% and 23%) with higher cell harvest concentrations (2.4 and 16.0 g/L), highlighting a trade off between bioethanol productivity and cell concentration in the harvest.

Also, the highest dilution rate of 0.58 h^{-1} reached a 6.5 g/L/h productivity with a higher efficiency in the glucose uptake (94%). Moreover, operating at high dilution rates prevents substrate and product inhibition (Karapatsia et al., 2016), as seen in the low ethanol concentrations (< 23 g/L). While significant margin for optimization of bioethanol production exists, the benefits of cell retention may also be beneficial for other high-value fermentation products.

5. Conclusions

This study reveals for the first time the benefits of ultrasonic cell retention for bioethanol production. A laboratory scale fermenter was operated at higher than the maximum specific growth rate for anaerobic glucose fermentation. The productivity of ethanol was significantly higher than reported batch or fed-batch systems due to the high cell concentration (8.8 ± 0.9 g/L/h). We present a Response Surface Model that predicts the separation efficiency of ultrasonic sedimentation of yeast cells, with main and interaction effects. The model was calibrated from a Central Composite Faced experimental design ($R^2_{validation} = 0.81$). Ultrasonic yeast sedimentation is a promising technology for cell retention and enhanced productivity in continuous fermentation processes.

Declaration of Competing Interest

The authors declare no conflicts of interest. The funders had no role in the design of the study; in the collection, analyses, or interpretation of data; in the writing of the manuscript, or in the decision to publish the results.

Acknowledgements

This work was funded by the Novo Nordisk Foundation within the framework of the Fermentation-based Biomanufacturing Initiative (FBM), grant number NNF17SA0031362.

Appendix A. Supporting information

Supplementary data associated with this article can be found in the online version at doi:10.1016/j.fbp.2023.06.002.

References

Balat, M., 2011. Production of bioethanol from lignocellulosic materials via the biochemical pathway: A review. Energy Convers. Manag 52, 858–875. https://doi.org/10.1016/j.enconman.2010.08.013

Bosma, R., van Spronsen, W.A., Tramper, J., Wijffels, R.H., 2003. Ultrasound, a new separation technique to harvest microalgae. J. Appl. Phycol. 15, 143–153. https://doi.org/10.1023/A:1023807011027

Brandberg, T., Karimi, K., Taherzadeh, M.J., Franzén, C.J., Gustafsson, L., 2007. Continuous fermentation of wheat-supplemented lignocellulose hydrolysate with different types of cell retention. Biotechnol. Bioeng. 98, 80–90. https://doi.org/10.1002/bit.21410

Chang, Y.-H., Chang, K.-S., Chen, C.-Y., Hsu, C.-L., Chang, T.-C., Jang, H.-D., 2018. Enhancement of the Efficiency of Bioethanol Production by Saccharomyces cerevisiae via Gradually Batch-Wise and Fed-Batch Increasing the Glucose Concentration. Fermentation 4, 45. https://doi.org/10.3390/fermentation4020045

Chen, L.-J., Xu, Y.-L., Bai, F.-W., Anderson, W.A., Moo-Young, M., 2005. Observed quasi-steady kinetics of yeast cell growth and ethanol formation under very high gravity fermentation condition. Biotechnol. Bioprocess Eng. 10, 115–121. https://doi.org/10.1007/BF02932580

Fan, S., Xiao, Z., Zhang, Y., Tang, X., Chen, C., Li, W., Deng, Q., Yao, P., 2014. Enhanced ethanol fermentation in a pervaporation membrane bioreactor with the convenient permeate vapor recovery. Bioresour. Technol. 155, 229–234. https://doi.org/10.1016/j.biortech.2013.12.114

Hawkes, J.J., Coakley, W.T., 1996. A continuous flow ultrasonic cell-filtering method. Enzym. Microb. Technol. 19, 57–62. https://doi.org/10.1016/0141-0229(95)00172-7

Hawkes, J.J., Limaye, M.S., Coakley, W.T., 1997. Filtration of bacteria and yeast by ultrasound-enhanced sedimentation. J. Appl. Microbiol 82, 39–47. https://doi.org/10.1111/j.1365-2672.1997.tb03295.x

He, R., Ren, W., Xiang, J., Dabbour, M., Kumah Mintah, B., Li, Y., Ma, H., 2021. Fermentation of Saccharomyces cerevisiae in a 7.5 L ultrasound-enhanced fermenter: Effect of sonication conditions on ethanol production, intracellular Ca2+ concentration and key regulating enzyme activity in glycolysis. Ultrason. Sonochem. 76, 105624. https://doi.org/10.1016/j.ultsonch.2021.105624

Huezo, L., Shah, A., Michel, F., 2019. Effects of ultrasound on fermentation of glucose to ethanol by Saccharomyces cerevisiae. Fermentation 5, 16. https://doi.org/10.3390/fermentation5010016

Karapatsia, A., Penloglou, G., Chatzidoukas, C., Kiparissides, C., 2016. Fed-batch Saccharomyces cerevisiae fermentation of hydrolysate sugars: A dynamic model-based approach for high yield ethanol production. Biomass Bioenergy 90, 32–41. https://doi.org/10.1016/j.biombioe.2016.03.021

Kumar, S., Singh, S.P., Mishra, I.M., Adhikari, D.K., 2011. Continuous ethanol production by Kluyveromyces sp. IIPE453 immobilized on bagasse chips in packed bed reactor. J. Pet. Technol. 2, 1–6.

Ling, C., Qiao, G., Shuai, B., Song, K., Yao, W., Jiang, X., Chen, G., 2018. Engineering self-flocculating halomonas campaniensis for wastewaterless open and continuous fermentation. Biotechnol. Bioeng. 116, bit.26897. https://doi.org/10.1002/bit.26897

Li, T., Chen, X., Chen, J., Wu, Q., Chen, G.-Q., 2014. Open and continuous fermentation: Products, conditions and bioprocess economy. Biotechnol. J. 9, 1503–1511. https://doi.org/10.1002/biot.201400084

Li, S.-Y., Srivastava, R., Suib, S.L., Li, Y., Parnas, R.S., 2011. Performance of batch, fed-batch, and continuous A–B–E fermentation with pH-control. Bioresour. Technol. 102, 4241–4250. https://doi.org/10.1016/j.biortech.2010.12.078

Luo, X., Cao, J., Gong, H., Yan, H., He, L., 2018. Phase separation technology based on ultrasonic standing waves: A review. Ultrason. Sonochem. 48, 287–298. https://doi.org/10.1016/j.ultsonch.2018.06.006

Mohd Azhar, S.H., Abdulla, R., Jambo, S.A., Marbawi, H., Gansau, J.A., Mohd Faik, A.A., Rodrigues, K.F., 2017. Yeasts in sustainable bioethanol production: A review. Biochem. Biophys. Rep. 10, 52–61. https://doi.org/10.1016/j.bbrep.2017.03.003

Palme, O., Comanescu, G., Stoineva, I., Radel, S., Benes, E., Develter, D., Wray, V., Lang, S., 2010. Sophorolipids from Candida bombicola: Cell separation by ultrasonic particle manipulation. Eur. J. Lipid Sci. Technol. 112, 663–673. https://doi.org/10.1002/ejlt.200900163

Radel, S., McLoughlin, A.J., Gherardini, L., Doblhoff-Dier, O., Benes, E., 2000. Viability of yeast cells in well controlled propagating and standing ultrasonic plane waves. Ultrasonics 38, 633–637. https://doi.org/10.1016/S0041-624X(99)00211-5

Rahimi, A., Hosseini, S.N., Karimi, A., Aghdasinia, H., Arabi Mianroodi, R., 2019. Enhancing the efficiency of recombinant hepatitis B surface antigen production in Pichia pastoris by employing continuous fermentation. Biochem. Eng. J. 141, 112–119. https://doi.org/10.1016/j.bej.2018.10.019

Rattanapan, A., Limtong, S., Phisalaphong, M., 2011. Ethanol production by repeated batch and continuous fermentations of blackstrap molasses using immobilized yeast cells on thin-shell silk cocoons. Appl. Energy 88, 4400–4404. https://doi.org/10.1016/j.apenergy.2011.05.020

Saha, K., Maharana, A., Sikder, J., Chakraborty, S., Curcio, S., Drioli, E., 2019. Continuous production of bioethanol from sugarcane bagasse and downstream purification using membrane integrated bioreactor. Catal. Today 331, 68–77. https://doi.org/10.1016/j.cattod.2017.11.031

Sánchez, Ó.J., Cardona, C.A., 2008. Trends in biotechnological production of fuel ethanol from different feedstocks. Bioresour. Technol. 99, 5270–5295. https://doi.org/10.1016/j.biortech.2007.11.013

Shin, M.K., Park, K., Cho, G.H., 1999. Ultrasonic cell separator as a cell retaining device for high density cultures of plant cell. Biotechnol. Bioprocess Eng. 4, 264–268. https://doi.org/10.1007/BF02933750

Singh, S., Sarma, S., Agarwal, M., Goyal, A., Moholkar, V.S., 2015. Ultrasound enhanced ethanol production from Parthenium hysterophorus: A mechanistic investigation. Bioresour. Technol. 188, 287–294. https://doi.org/10.1016/j.biortech.2014.12.038

Tse, T.J., Wiens, D.J., Reaney, M.J.T., 2021. Production of bioethanol—a review of factors affecting ethanol yield. Fermentation 7, 1–18. https://doi.org/10.3390/fermentation7040268

de Vasconcelos, J.N., Lopes, C.E., de França, F.P., 2004. Continuous ethanol production using yeast immobilized on sugar-cane stalks. Braz. J. Chem. Eng. 21, 357–365. https://doi.org/10.1590/S0104-66322004000300002

Wu, M., Ouyang, Y., Wang, Z., Zhang, R., Huang, P.-H., Chen, C., Li, H., Li, P., Quinn, D., Dao, M., Suresh, S., Sadovsky, Y., Huang, T.J., 2017. Isolation of exosomes from whole blood by integrating acoustics and microfluidics. Proc. Natl. Acad. Sci. 114, 10584–10589. https://doi.org/10.1073/pnas.1709210114

Wu, M., Ozcelik, A., Rufo, J., Wang, Z., Fang, R., Jun Huang, T., 2019. Acoustofluidic separation of cells and particles.

Microsyst. Nanoeng. 5, 32. https://doi.org/10.1038/s41378-019-0064-3

Xie, D., Miller, E., Sharpe, P., Jackson, E., Zhu, Q., 2017. Omega-3 production by fermentation of Yarrowia lipolytica: From fed-batch to continuous. Biotechnol. Bioeng. 114, 798–812. https://doi.org/10.1002/bit.26216

Zhang, Q., Wu, D., Lin, Y., Wang, X., Kong, H., Tanaka, S., 2015. Substrate and product inhibition on yeast performance in ethanol fermentation. Energy Fuels 29, 1019–1027. https://doi.org/10.1021/ef502349v

Zhang, L., Zhao, H., Gan, M., Jin, Y., Gao, X., Chen, Q., Guan, J., Wang, Z., 2011. Application of simultaneous saccharification and fermentation (SSF) from viscosity reducing of raw sweet potato for bioethanol production at laboratory, pilot and industrial scales. Bioresour. Technol. 102, 4573–4579. https://doi.org/10.1016/j.biortech.2010.12.115

Zheng, C., Sun, X., Li, L., Guan, N., 2012. Scaling up of ethanol production from sugar molasses using yeast immobilized with alginate-based MCM-41 mesoporous zeolite composite carrier. Bioresour. Technol. 115, 208–214. https://doi.org/10.1016/j.biortech.2011.11.056